Progress In Electromagnetics Research C, Vol. 122, 153–164, 2022

Synthesizing Radiation Properties of Dual-Band Dual-Mode High Gain Dielectric Resonator Antenna for Wireless Applications

Juin Acharjee[1], Shreya Chatterjee[1], Nipun K. Mishra[2, *], Gouri S. Paul[3], and Kaushik Mandal[4]

Abstract—In this article, the radiation properties of a slot-loaded cylindrical dielectric resonator antenna (CDRA) have been analyzed strategically to realize a dual-band operation with a higher gain. A microstrip line based aperture coupled feed is adopted to excite dual modes at 4.8 GHz and 8.28 GHz with an impedance bandwidth of 5.84% (280 MHz) and 10.62% (880 MHz), respectively. A superstrate layer is placed at a suitable gap above the antenna structure to enhance the antenna gain by utilizing the principle of multiple reflections. For the further improvement of gain, a plus-shaped slot is incorporated on the superstrate that helps to concentrate the radiated field at the center of the superstrate, thereby the directivity of the CDRA has been enhanced on a large scale. The proposed structure is fabricated and measured for experimental verification that demonstrate 3 dB augmentations in antenna peak gain in comparison to the conventional CDRA. The experimental result shows a good agreement with the simulated ones. Higher measured peak gains of 7.87 dBi and 7.91 dBi at two operating bands ensure the applicability of the proposed simple structure for high gain wireless applications.

1. INTRODUCTION

Dielectric resonator antenna (DRA) is widely used in different emerging applications for its several features like high gain, low dielectric loss, and wide bandwidth [1, 2]. Many shapes of DRA like rectangle [3], hemisphere [4], cylinder [5–8], etc. have been investigated with probe feed [9], micro-strip feed [10], aperture coupled techniques [11–16], and other feeding techniques for various applications. For modern long-distance communications, there is always a requirement of a high gain antenna with some additional features which are not feasible by using a traditional DRA. So the traditional concept of array design [2] is deployed by the engineers. This method is not suitable for all applications due to the limitation of the compact installation platform. Therefore to solve these issues, varieties of gain enhancement techniques, such as the use of electromagnetic bandgap (EBG) structure [17], metallic cap [18], different feeding mechanisms [19], stacked configured of different layers [20], frequency selective surfaces (FSS) [21], and superstrate layer [22–26], are developed by researchers. In most of the reported articles, it is observed that the gain enhancement at the lower frequencies by maintaining the miniaturized dimension becomes a challenging task. In [17], a millimeter-wave DRA surrounded by an EBG structure increases the gain up to 3.2 dBi. In [18], with the increment of the radius of the metallic cap, the gain is enhanced up to 8.54 dBi. The same DRA structure can be used to excite different modes by applying different feeding techniques. As explained in [19], one of the common techniques is the use of a coplanar waveguide feeding, which can directly generate a wide bandwidth

Received 31 May 2022, Accepted 26 July 2022, Scheduled 9 August 2022

* Corresponding author: Nipun Kumar Mishra (mishranipun@gmail.com).

[1] Department of Electronics & Communication Engineering, ST. Thomas' College of Engineering & Technology, Kolkata 700023, West Bengal, India. [2] Guru Ghasidas Vishwa vidyalaya (Central University), Bilaspur, India. [3] Global Institute of Science and Technology, Haldia, West Bengal, India. [4] Department of Radio Physics and Electronics, University of Calcutta, 92 A. P. C Road, Kolkata 700009, West Bengal, India.

with boresight radiation characteristics of DRA. Using a cylindrical dielectric resonator (CDR), an intermediate layer, and a metallic cylinder together, significant improvement of bandwidth and gain can be achieved by minimizing surface wave [20]. The use of a dual-band FSS with bandpass response as a superstrate above the DRA is one of the reported techniques for gain improvement in both the operating bands [21]. Dual-band characteristics in superstrate loaded cylindrical DRA are reported with enhanced gain performance [22], whereas by placing a thin dielectric material as intermediate layer between antenna and feed network along with dielectric material as superstrate at top of radiator [23], the combination of superstrate with reflector [24] can be used to design a wideband DRA with improved gain characteristics. Though all these techniques [17–20] are very effective for the gain improvement of the traditional DRA, sometimes dealing with different challenging issues like stacking of different layers, precision fabrication, etc., improper arrangements or modifications in the DRA structure may lead to affecting the quality factor. The techniques summarized in [21–24] improve the radiation characteristics without much affecting the other performances, but investigation on these techniques is limited, which needs to be extended further.

In this work, an aperture coupled feed conventional CDRA is designed as a reference antenna to operate at two bands. For the gain enhancement of this reference antenna, the electric field distributions on the superstrate layer have been analyzed thoroughly by strategic choice and placement of slots. Instead of using a single horizontal or vertical rectangular slot, symmetric placement of a plus-shaped slot at the center position forces the electric field vectors to concentrate at the center of the superstrate. It makes the CDRA unique and competent. The design methodology of the proposed antenna is discussed in Section 2 followed by the discussion on the analysis of radiation properties of the antenna for the gain enhancement. Validation of the simulated result is discussed in Section 3 followed by the concluding remarks in Section 4. All the characteristics of the proposed composite structure are analyzed using FEM-based Ansys HFSS EM simulator V.19.

2. ANTENNA DESIGN AND ANALYSIS

2.1. Antenna Configuration

Figure 1 shows the detailed construction of the proposed CDRA with a superstrate layer. Construction is based on an FR4 substrate of dimension $62\times62\,\text{mm}^2$, dielectric constant $(\varepsilon_r) = 4.4$, height $(h) = 1.6\,\text{mm}$, and loss tangent $(\tan\delta) = 0.02$. A cylinder-shaped dielectric resonator (DR) made of Arlon of radius (r_d) 10.5 mm and height (h_d) 7 mm with $\varepsilon_d = 10.7$ is placed exactly at the center of the FR4 substrate and a rectangular aperture of length 14 mm and width 3.7 mm on the top side of the substrate. The CDRA is excited by a microstrip line of length 34 mm and width 3 mm embedded at the bottom side of the substrate. Indirect feeding methodology is applied in the structure to feed the CDRA through the slot. For improving the gain of the CDRA, a metallic superstrate (45 mm × 45 mm) is printed on the

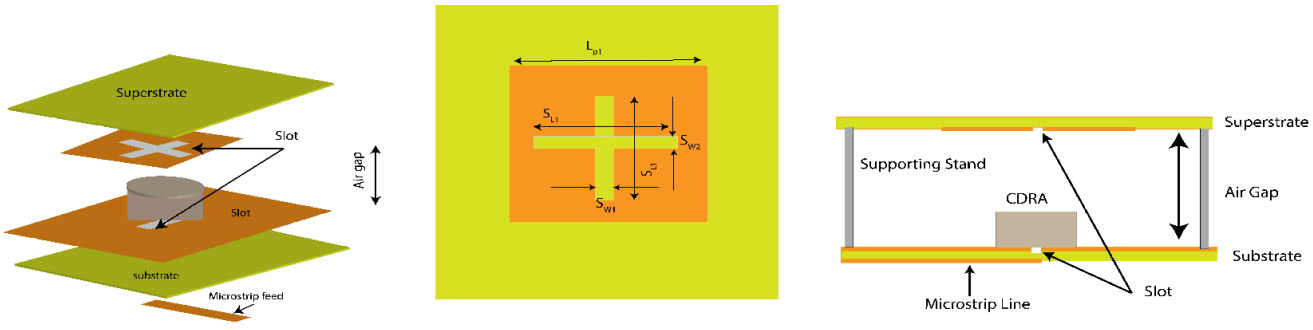

Figure 1. Structures of the proposed aperture coupled CDRA fed by a microstrip line: (a) perspective view, (b) bottom view of the superstrate, and (c) side view, [Dimensions of the optimized parameters $L_{P1} = 45\,\text{mm}$, $S_{W2} = 3.2\,\text{mm}$, $S_{L1} = 32\,\text{mm}$, $S_{W1} = 3.4\,\text{mm}$, $h_{eff} = 30\,\text{mm}$].

bottom side of the FR4 superstrate (62 mm × 62 mm × 1.6 mm). This superstrate layer is placed at an air gap of 30 mm from the top of the lower substrate. After careful analysis of electric field distributions on the surface of the unmodified superstrate, a plus-shaped slot is embedded symmetrically at the center of the superstrate layer to concentrate the electric fields at the center position, which helps to enhance the directivity of the conventional CDRA.

2.2. Antenna Design Methodology

The reference CDRA is designed for the fundamental hybrid mode $HEM_{11\delta}$ using (1), as described in [25]

$$f_r(\mathrm{HEM}_{11\delta}) = \frac{c}{2\pi r_d} \times \frac{6.324}{\sqrt{\varepsilon_d + 2}} \times \left[0.27 + 0.36\left(\frac{r_d}{2h_d}\right) + 0.02\left(\frac{r_d}{2h_d}\right)^2\right]. \quad (1)$$

where c = velocity of light, ε_d = permittivity of the cylindrical DRA, r_d = radius of the cylindrical DRA, h_d = height of the cylindrical DRA.

In the design, the aperture coupled feeding technique is adopted to excite multiple modes. After proper optimization of the height and radius of the slot coupled CDRA, dual-mode is excited, and the corresponding modes are identified, as shown in Figure 2. Resonances at both the modes are justified with the proper impedance matching where real and imaginary impedances attain the values (R_{in}) 48.7 Ω, 51.9 Ω and (X_{in}) 0.9 and 0.98, respectively, as shown in Figure 3.

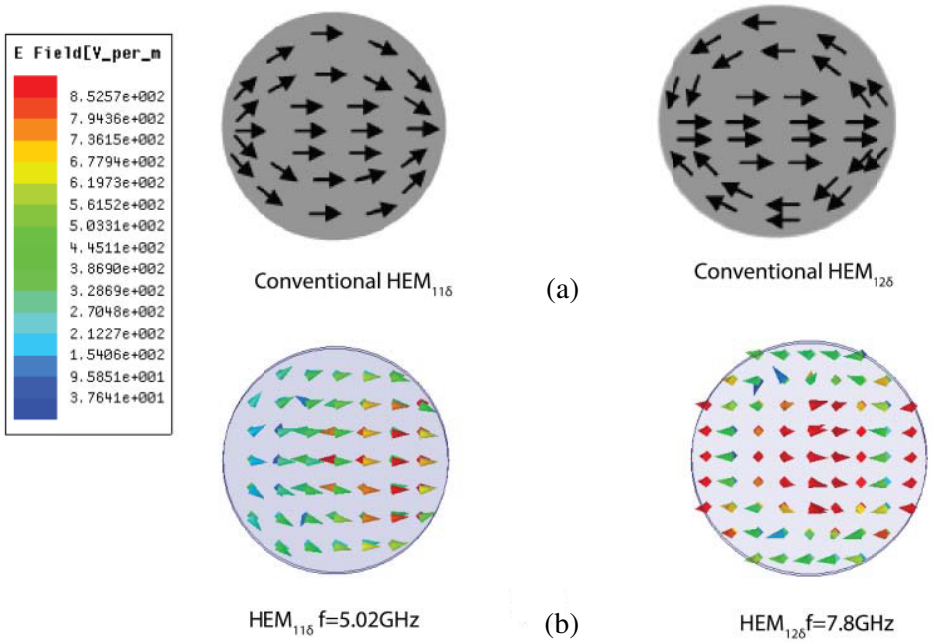

Figure 2. (a) Conventional modes of CDRA. (b) Identification of the generated mode for the proposed CDRA.

2.3. Parametric Studies

There are some crucial design parameters, like the length and position of the coupling slot, which directly affect the performance of the CDRA. Therefore, some parametric studies are carried out to determine their effect and to optimize the design parameters.

2.3.1. Ground Slot Length (S_{L2}) Variation

Figure 4 shows the effect on the reflection coefficient (S_{11}) for the variation of length of the coupling slot embedded beneath the CDR. When the length of the slot is chosen as 12 mm, no proper impedance

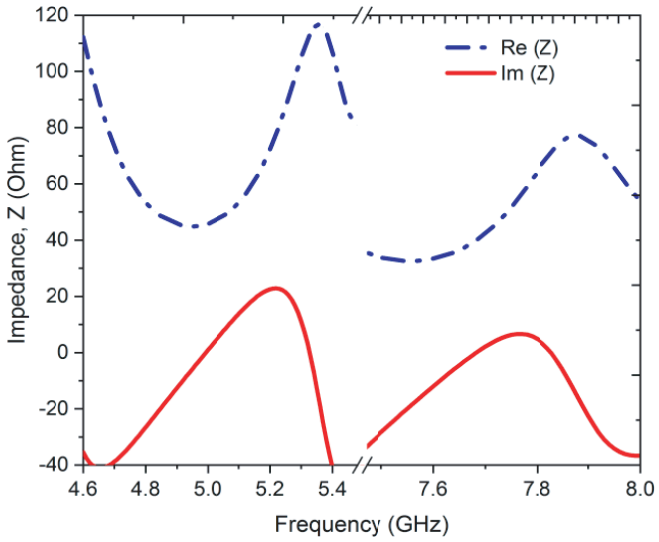

Figure 3. Impedance variation of proposed CDRA at both the resonating frequencies.

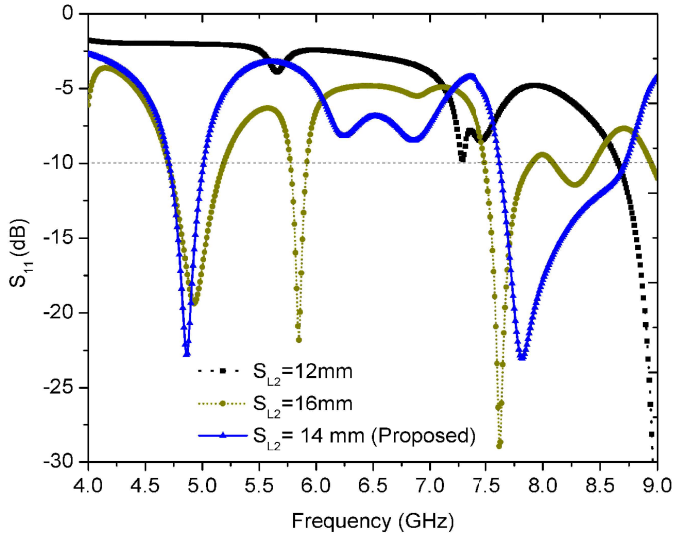

Figure 4. Simulated reflection coefficients for the length variation of coupling slot.

matching is observed throughout the band, whereas for $S_{L2} = 16$ mm, triple band resonating behavior is observed where all the resonances are not radiating in nature. Finally, the slot length has been settled at 14 mm, for which wide impedance bandwidth at both the operating bands is realized with excellent impedance matching.

2.3.2. Angular Variation of Coupling Slot

The effects on S_{11} due to angular rotation of the coupling slot with respect to the CDR are summarized in Figure 5. For the orthogonal orientation of the slot (i.e., just above the feed line) with reference to the proposed orientation, resonance at both the operating bands vanishes. Due to the right rotational movement of the slot, impedance matching at second resonance degraded, whereas for the left rotational movement first and second, both the resonating bands shifted to the higher frequency range with poor impedance matching. For the proposed position only, more coupling of fields between the microstrip line and CDR occurs; as a result, dual-band behavior with good impedance matching is obtained.

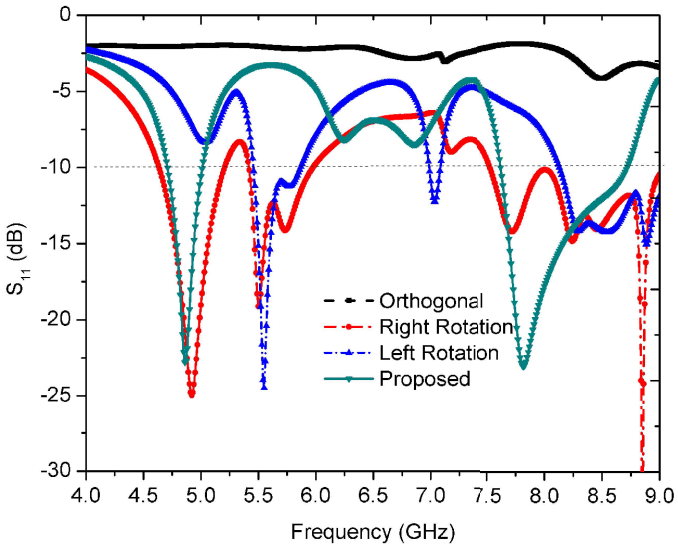

Figure 5. Simulated reflection coefficients for the orientation variation of the coupling slot on the ground plane.

3. ENHANCEMENT OF GAIN USING SUPERSTRATE LAYER

A superstrate layer is used widely to enhance antenna gain. Enhancement of antenna gain using a superstrate layer is based on the principle of multiple reflections [26]. Proper placement of the superstrate layer ensures that most of the radiating waves penetrate the superstrate, and some of the waves are reflected. In the second round, these reflected waves are combined with the transmitted waves and become the strongest to penetrate the superstrate layer more effectively. It helps to enhance the directivity further. Now the performances of the proposed superstrate layer are investigated, and the transmission and reflection responses are plotted in Figure 6. It can be observed that this superstrate exhibits two passbands across 4.5–5.24 GHz and 7.58–8.57 GHz, with transmission poles at 4.8 GHz and 7.8 GHz, respectively. Therefore, the proposed superstrate layer shows a transparent nature in two frequency bands in which the proposed DRA operates. For further clarification of insertion of the slot

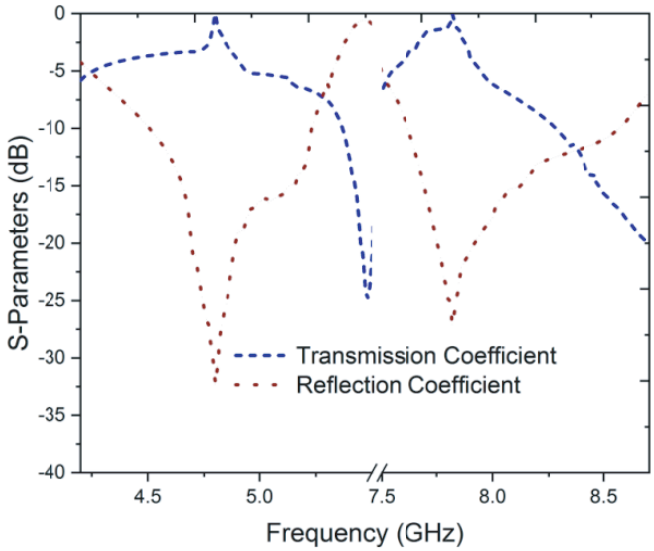

Figure 6. Simulated reflection and transmission coefficient of the slot loaded superstrate layer.

for further gain enhancement of the reference CDRA, the electric field distributions (Figure 7) on the superstrate layer have been analyzed thoroughly and synthesized by strategic choice and placement of slots. Instead of using a single horizontal or vertical rectangular slot, the symmetric placement of a plus-shaped slot at the center position forces the electric field vectors to concentrate at the center of the superstrate.

It helps to produce more directive radiation patterns at both the operating bands. A pictorial representation of that concentrated electric field at the center of the superstrate layer is shown in Figure 7. Figures 7(a) and (b) show that a strong peak (magnitude of electric field) at the centre is

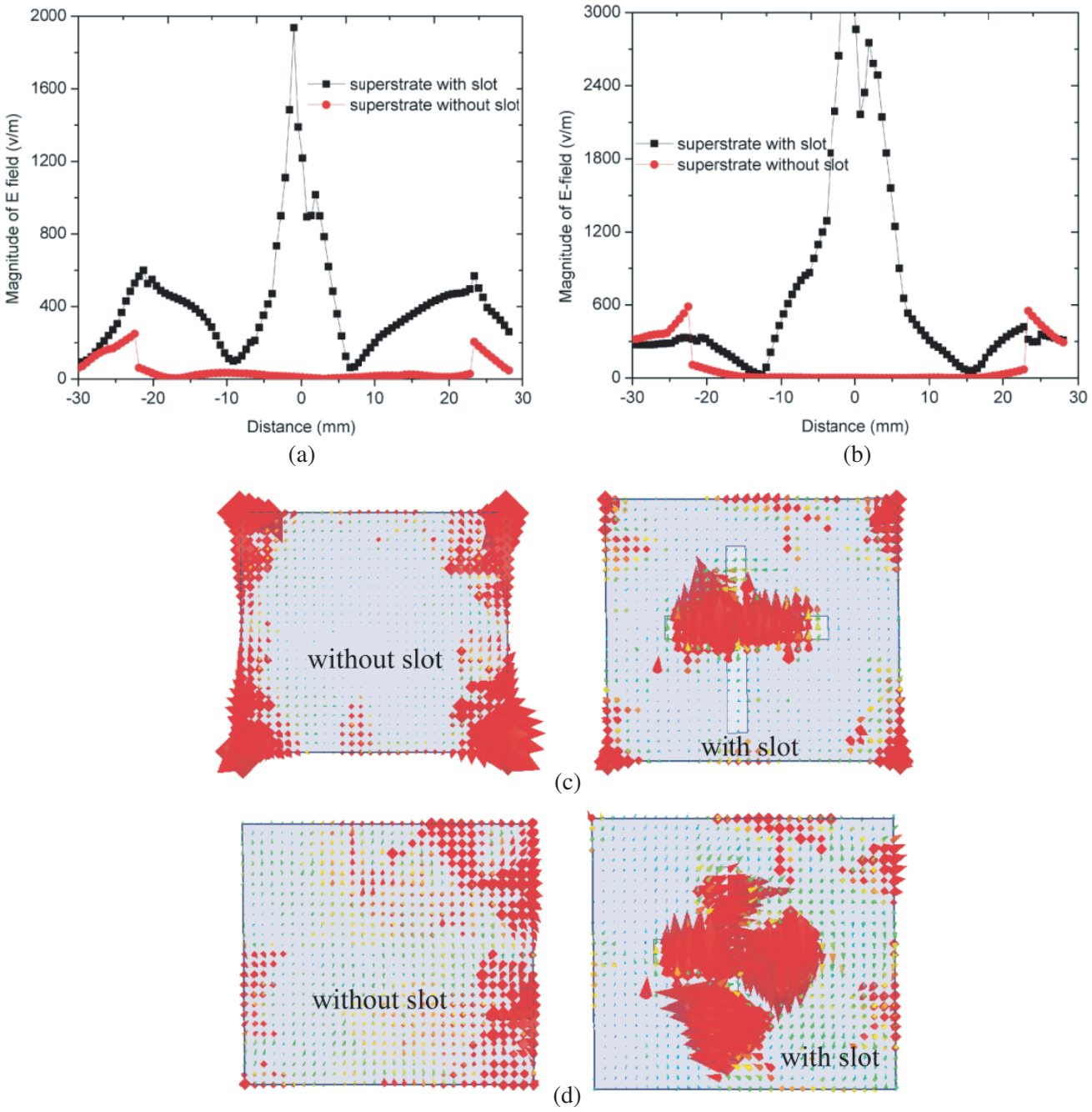

Figure 7. Plots of electric field magnitude on the superstrate at (a) 4.8 GHz, and (b) 8.28 GHz; and the simulated electric field vector portrayals at (c) 4.8 GHz and (d) 8.28 GHz.

observed in the presence of slot for both the frequencies. The electric field vectors with and without plus-shaped slot are also shown in Figures 7(c) and 7(d) for both frequencies. The symmetrical placement of the slot forces electric field vectors to concentrate at the center, which ensures the enhancement of the directivity of the CDRA.

The position of the superstrate layer is fixed following (2) to make the gap permissible for multiple reflections

$$h_{super} = c/2f_0 \tag{2}$$

where c is the velocity of light in free space, and f_0 is lower resonating frequency.

A combination of superstrate with dielectric resonator closely forms a Fabry-Perot cavity [25]. Therefore, the effective gap between two walls of cavity formed by superstrate and base of the dielectric resonator can be calculated using (3).

$$h_{eff} = \sqrt{\varepsilon_{eff}} h_{super} \tag{3}$$

where ε_{eff} is the effective permittivity of the cavity. Due to the presence of DR and air inside the cavity, ε_{eff} can be calculated using (4) [25]

$$\sqrt{\varepsilon_{eff}} = \sqrt{\frac{h_d + (h_{super} - h_d)}{(h_d/\varepsilon_r) + (h_{super} - h_d)}} \tag{4}$$

where h_d is the height of the dielectric resonator.

Therefore as per the calculated value, the superstrate layer is placed at an air gap of $\lambda/2$, for getting higher directivity.

The effects of proper positioning of the superstrate layer on reflection coefficient and gain variation are shown in Figures 8(a) and 8(b), respectively. Figure 8(a) shows that the placement of the superstrate layer at a distance of $\lambda/2.5$ deteriorates the impedance matching at the first resonance and bandwidth of the second operating band. For a distance of $\lambda/3$, shift the first resonance toward the higher frequency and decrease the bandwidth of the second band. The position of superstrate layer other than the calculated distance ($\lambda/2$) shows either constant gain variation or degradation of gain in both the operating bands. Therefore, proper placement of the superstrate layer shows good impedance matching behavior as well as the antenna gain enhancement in both the operating bands. Moreover, it is also observed that the reflection coefficient is not much affected due to the proper placement of this superstrate layer.

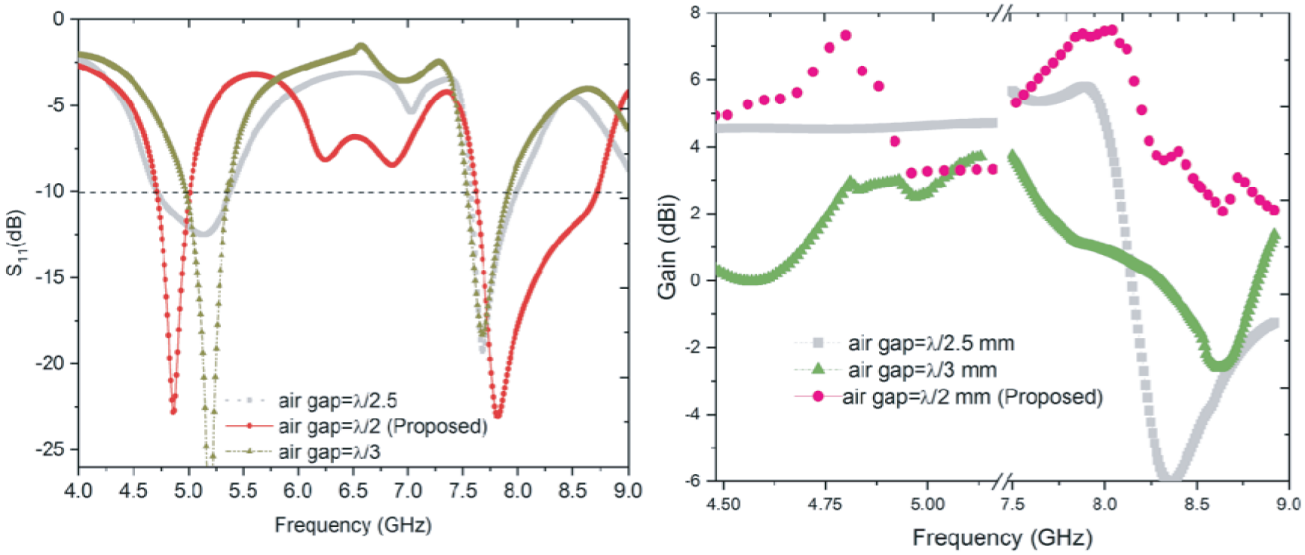

(a) (b)

Figure 8. Variation of air gap between superstrate and the base of CDRA: (a) simulated S_{11}, and (b) simulated peak gain at the operating bands.

4. RESULT AND DISCUSSION

The prototypes are fabricated and assembled carefully to realize the composite structure of the proposed design. Photographs of this composite structure are shown in the inset of Figure 9. A comparison of simulated and measured reflection coefficients and gains is shown in Figure 9. Acceptable agreement between the simulated and measured results is observed. A slight mismatch in the second operating band may be due to the fabrication tolerances. The measured S_{11} shows ≤ -10 dB impedance bandwidth across 4.64–4.92 GHz and 7.84–8.72 GHz frequency bands with resonances at 4.8 GHz and 8.28 GHz, respectively.

Radiation patterns at both the principal planes with and without superstrate layer are shown in

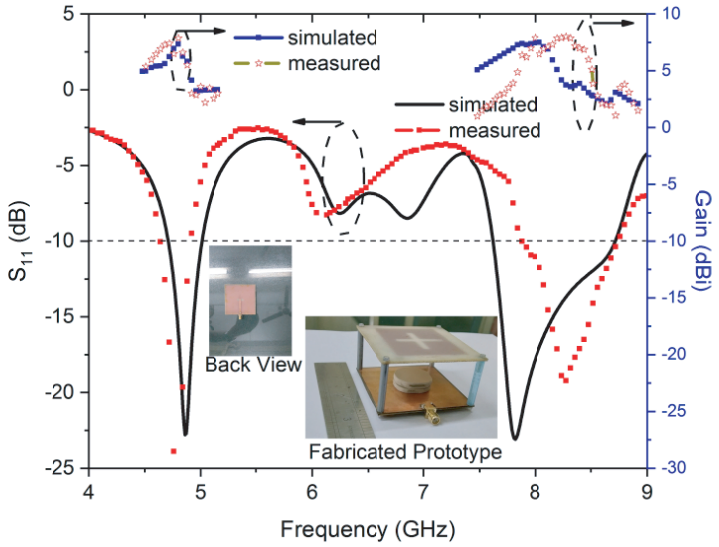

Figure 9. Simulated and measured reflection coefficients (S_{11}) and gains, and photos of the fabricated prototype.

Table 1. Comparison of the proposed structure with some previously reported high gain DRA.

Ref. No.	Methodology Used	Overall Dimension (correspond to the higher resonating frequency) (mm^2)	Mea. $\lvert\Gamma_{in}\rvert$ (dB)	BW (%)	Peak XP Level (dB)		No. of operating bands	Mea. Peak Gain (dBi)	*E*-plane beamwidth	
					$\Phi = 0°$	$\Phi = 90°$			1st band	2nd band
[16]	Slotted ground	$1.39\lambda_0 \times 1.39\lambda_0$	-32	1.56	-23	-21	1	9.62	36°	52°
[21]	Frequency selective surface	$1.06\lambda_0 \times 1.06\lambda_0$	-14 / -35	6.5/ 16.95	≈ -27	≈ -27	2	7.5, 10.95	74°	60°
[22]	Superstrate layer	$1.12\lambda_0 \times 1.12\lambda_0$	≈ -17 / ≈ 12	5.4/ 5.76	≈ -22	≈ -21	2	8, 7.8	NM	NM
[23]	Incorporating superstrate layer	$1.70\lambda_0 \times 1.70\lambda_0$	max. ≈ 25	23	≈ -90	≈ -23	1	11	NM	NM
Pro.	Slotted superstrate layer	$1.2\lambda_0 \times 1.2\lambda_0$	-24.8 / -20	5.84/ 10.63	≈ -25	-15	2	7.87, 7.91	32°	38°

NM: Not Mentioned; λ_0: Free space wavelength of the corresponding higher resonating frequency.

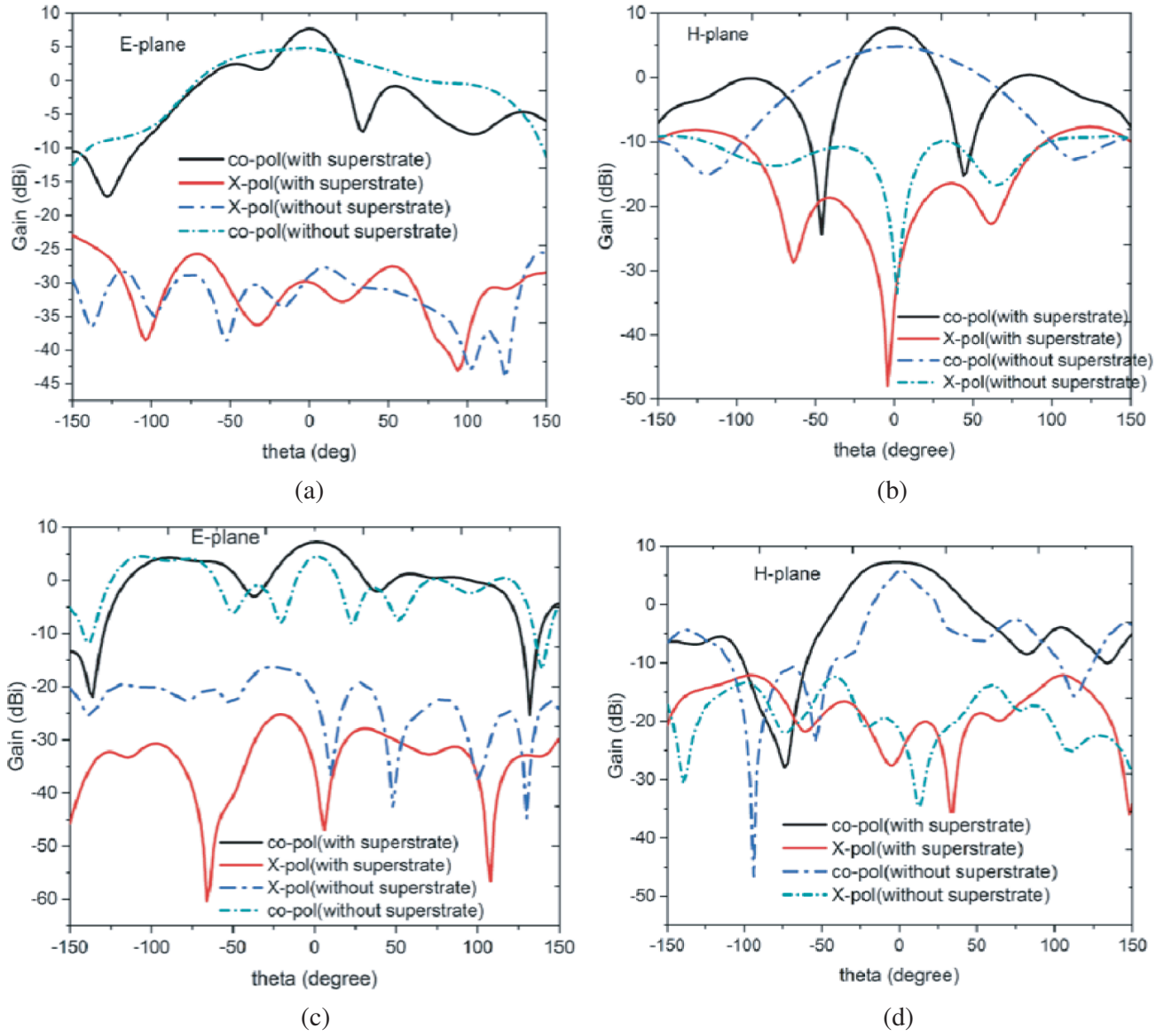

Figure 10. Simulated radiation patterns, (a) E-plane, (b) H-plane at 4.8 GHz, and (c) E-plane, (d) H-plane at 8.28 GHz.

Figure 10. It shows a co-polarization (co-pol) to cross-polarization (XP) isolation (polarization purity) more than 20 dB at both the planes for both resonating frequencies. The H-plane pattern at the first resonating frequency exhibits an XP reduction of 5 dB. At the second resonance, the XP reductions is not significant due to the presence of more orthogonal fields, which are not shown here for brevity. The co-pol patterns in both the principal planes are directive at both the operating bands. In the lower band, the 3-dB beamwidths of the proposed design at the E-plane and H-plane are 32° and 40°, respectively, whereas in the upper band, the beamwidths become 38° and 56°, respectively. Measured peak gains at the two operating bands are 7.87 dBi and 7.91 dBi, respectively. The 3-D radiation patterns are shown in Figure 11 to visualize the generation of highly directive patterns due to the inclusions of the slot-loaded superstrate layer.

In Table 1, the performances of the proposed CDRA are compared with some earlier reported wideband high gain DRA designs. The first point to observe is that the proposed model is superior to both the designs in [16] and [23] in terms of dimension, the number of operating bands, and beam width.

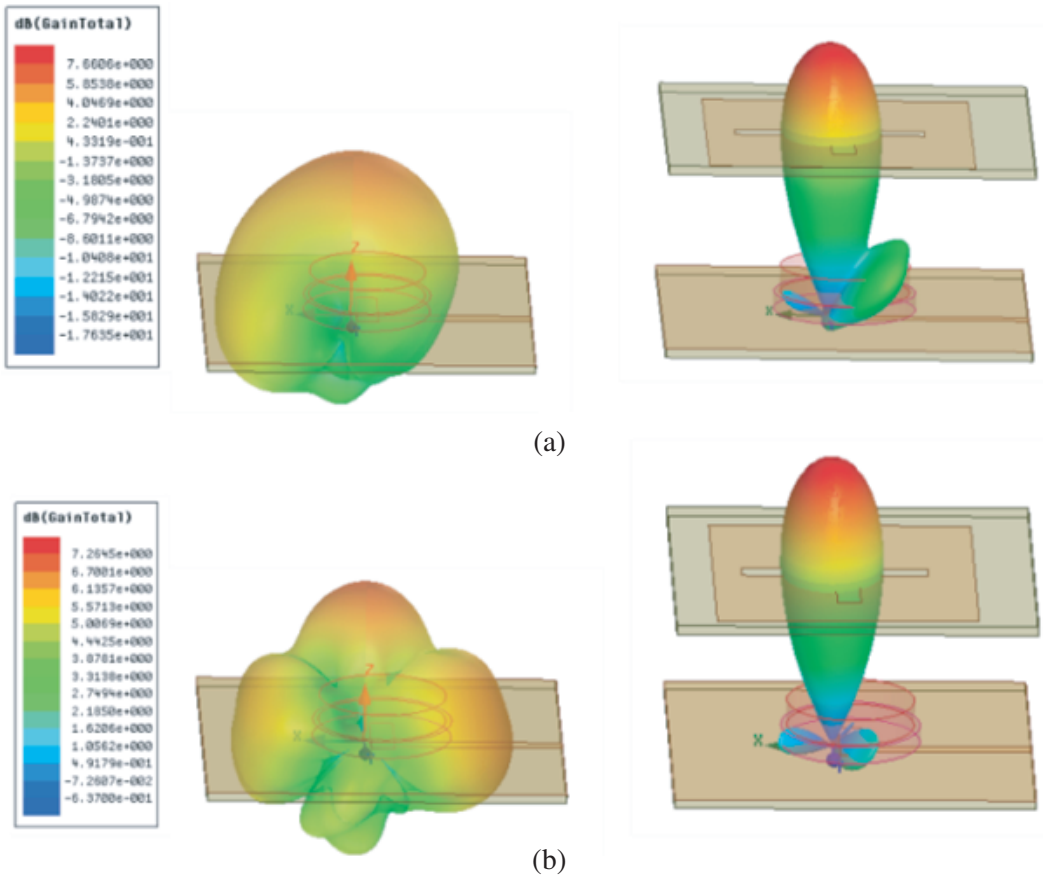

Figure 11. 3-D Polar plot with and without superstarte layer at (a) 4.8 GHz, and (b) 8.28 GHz.

The gain and bandwidth of the antenna in [23] are higher than the proposed model, as the former uses a DRA made with a lower permittivity value of ($\varepsilon_r = 6.15$). Secondly, the proposed model is superior to [21] and [22] in terms of impedance matching and beamwidth. Therefore, performances of the proposed model shows significant improvement in terms of good impedance matching, low beamwidth, optimized bandwidth, stable high gain, and optimized peak XP level at both the operating bands compared to previously reported articles.

5. CONCLUSION

An aperture coupled feed dual-band CDRA has been integrated with a slot-loaded superstrate to produce highly directive patterns at both the operating bands. Excitation of two modes and the best coupling between the feed line and DR is ensured by the proper placement of the rectangular-shaped coupling slot beneath the DR. Further, the strategic inclusion of a plus-shaped slot on the superstrate and the appropriate placement of this superstrate gather all the electric fields mainly across the CDRA footprint, which helps to enhance the peak gain of the conventional CDRA in a large scale. The high peak gains, adequate operating bandwidth, and suitable directive patterns make this dual-band CDRA a potential design for practical wireless applications.

REFERENCES

1. Petosa, A., *Dielectric Resonator Antenna Handbook*, Artech House, 2007.
2. Petosa, A. and A. Ittipiboon, "Dielectric resonator antenna: A historical review and the current state of art," *IEEE Antennas Propag. Mag.*, Vol. 52, No. 5, 91–116, October 2010.

3. Mongia, R. K. and A. Ittipoboon, "Theoretical and experimental investigations on rectangular dielectric resonator antennas," *IEEE Trans. Antennas Propag.*, Vol. 45, No. 9, 1348–1356, 1997.
4. Mukherjee, B., V. D. Kumar, and M. Gupta, "A novel hemispherical dielectric resonator antenna on an electromagnetic band gap substrate for broadband and high gain systems," *AEU — International Journal of Electronics and Communications*, Vol. 68, 1185–1190, 2014.
5. Esmaeili, M. and J. J. Laurin, "Polarization reconfigurable slot-fed cylindrical dielectric resonator antenna," *Progress In Electromagnetics Research*, Vol. 168, 61–71, 2020.
6. Yang, W., A. Denidni, Q. Zeng, and G. Wei, "A wideband high-gain stacked cylindrical dielectric resonator antenna," *Progress In Electromagnetic Research Letters*, Vol. 53, 155–163, 2013.
7. Mishra, N. K., S. Das, and D. K. Vishwakarma, "Beam steered linear array of cylindrical dielectric resonator antenna," *AEU — International Journal of Electronics and Communications*, Vol. 98, 106–113, 2019.
8. Mishra, N. K., J. Acharjee, V. Sharma, C. Tamrakar, and L. Dewangan, "Mutual coupling reduction between the cylindrical dielectric resonator antenna using split ring resonator based structure," *AEU — International Journal of Electronics and Communications*, Vol. 154, 2022.
9. Huynh, A. P., D. R. Jackson, S. A. Long, and D. R. Wilton, "A Study of the impedance and pattern bandwidths of probe-fed cylindrical dielectric resonator antennas," *IEEE Antennas and Wireless Propag. Lett.*, Vol. 10, 1313–1316, 2011.
10. Bijumon, P. V., S. K. Menon, M. N. Suma, M. T. Sebastian, and P. Mohanan, "Broadband cylindrical dielectric resonator antenna excited by modified microstrip line," *Electronics Lett.*, Vol. 41, No. 7, March 2005.
11. O. G. Avădănei, M. G. Banciu, I. Nicolaescu, and L. Nedelcu, "Superior modes in high permittivity cylindrical dielectric resonator antenna excited by a central rectangular slot," *IEEE Transactions on Antennas and Propag.*, Vol. 60, No. 11, 5032–5038, November 2012.
12. Buerkle, A., K. Sarabandi, and H. Mosallaei, "Compact slot and dielectric resonator antenna with dual-resonance, broband characteristics," *IEEE Trans. on Antennas and Propag.*, Vol. 53, No. 03, 1020–1027, March 2005.
13. Mishra, N. K., S. Das, and D. K. Vishwakarma, "Low profile circularly polarized cylindrical dielectric resonator antenna coupled by L shaped resonating slot," *Microw. and Opt. Tech. Lett.*, Vol. 59, No. 05, 996–1000, 2017.
14. Mishra, N. K., S. Das, and D. K. Vishwakarma, "Bandwidth enhancement of cylindrical dielectric resonator antenna using thin dielectric layer fed by resonating slot," *Frequenz*, Vol. 70, No. 9–10, 381–388, 2016.
15. Buerkle, A., K. Sarabandi, and H. Mosallaei, "Compact slot and dielectric resonator antenna with dual-resonance, broband characteristics," *IEEE Trans. on Antennas and Propag.*, Vol. 53, No. 03, 1020–1027, March 2005.
16. Ojha, A. K. and P. Kumar, "High gain broadside mode operation of a cylindrical dielectric resonator antenna using simple slot excitation," *Int. Journal of Microw. and Wireless Tech.*, Vol. 13, No. 3, 286–294, 2021.
17. Al-Hasan, M. J., T. A. Denidni, and A. R. Sebak, "Millimeter-wave EBG-based aperture-coupled dielectric resonator antenna," *IEEE Trans. Antennas Propag.*, Vol. 61, No. 8, 4354–4357, August 2013.
18. Kim, T. and S. Pak, "Enhanced gain and miniaturization method of stacked dielectric resonator antenna using metallic cap," *IET Microwaves, Antennas & Propagation*, Vol. 13, No. 8, 1198–1201, July 2019.
19. Kumar, P., S. Dwari, S. Singh, J. Kumar, and A. Kumar, "Conductor backed CPW-fed dual-mode excited high gain cylindrical cavity DRA for Unmanned Aircraft Systems (UAS) or drone data-link applications at C band," *IETE Technical Review*, 1–11, 2018.
20. Wang, Y.-F., T. A. Denidni, Q.-S. Zeng, and G. Wei, "Design of high gain, broadband cylindrical dielectric resonator antenna," *Electronics Lett.*, Vol. 49, 1506–1507, 2013.

21. Ballav, S., A. Chatterjee, and S. K. Parui, "Gain augmentation of a dual-band dielectric resonator antenna with frequency selective surface superstrate," *International Journal of Microwave and Wireless Technologies*, Vol. 31, No. 8, 2021.
22. Dash, S. K., Q. S. Cheng, and T. Khan, "A superstrate loaded aperture coupled dual-band circularly polarized dielectric resonator antenna for X-band communications," *Int. Journal of Microw. and Wireless Tech.*, Vol. 13, 867–874, October 2020.
23. Mishra, N. K., S. Das, and D. K. Vishwakarma, "Wideband high gain cylindrical dielectric resonator antenna for X-band applications," *Frequenz*, Vol. 73, 109–116, 2019.
24. Dash, S. K. K. and T. Khan, "Wideband high gain conical dielectric resonator antenna: An experimental study of superstrate and reflector," *Int. Journal of Microw. and Wireless Tech.*, Vol. 27, 1–10, 2017.
25. Dutta, K., D. Guha, C. Kumar, and Y. M. Antar, "New approach in designing resonance cavity high-gain antenna using nontransparent conducting sheet as the superstrate," *IEEE Trans. on Antennas and Propag.*, Vol. 63, 2807–2813, 2015.
26. Munk, B. A., *Frequency Selective Surfaces: Theory and Design*, Wiley, New York, USA, 2000.